Article:

Berberoglu, S, Cilek, A, Kirkby, M et al. (2020) Spatial and temporal evaluation of soil erosion in Turkey under climate change scenarios using the Pan-European Soil Erosion Risk Assessment (PESERA) model. Environmental Monitoring and Assessment, 192 (8). 491. ISSN: 0167-6369

https://doi.org/10.1007/s10661-020-08429-5

Environ Monit Assess (2020) 192:491
https://doi.org/10.1007/s10661-020-08429-5

Spatial and temporal evaluation of soil erosion in Turkey under climate change scenarios using the Pan-European Soil Erosion Risk Assessment (PESERA) model

Suha Berberoglu · Ahmet Cilek · Mike Kirkby · Brian Irvine · Cenk Donmez

Received: 27 January 2020 / Accepted: 17 June 2020

Abstract The impacts of climate change on soil erosion are mainly caused by the changes in the amount and intensity of rainfall and rising temperature. The combination of rainfall and temperature change is likely to be accompanied by negative or positive variations in agricultural and forest management. Turkey contains vast fertile plains, high mountain chains and semi-arid lands, with a climate that ranges from marine to continental and therefore is susceptible to soil erosion under climate change, particularly on high gradients and in semi-arid areas. This study aims to model the soil erosion risk under climate change scenarios in Turkey using the Pan-European Soil Erosion Assessment (PESERA) model, predicting the likely effects of land use/cover and climate change on sediment transport and soil erosion in the country. For this purpose, PESERA was applied to estimate the monthly and annual soil loss for 12 land use/cover types in Turkey. The model inputs included 128 variables derived from soil, climate, land use/cover and topography data. The total soil loss from the land surface is speculated to be approximately 285.5 million tonnes per year. According to the IPCC 5th Assessment Report of four climate change scenarios, the total soil losses were predicted as 308.9, 323.5, 320.3 and 355.3 million tonnes for RCP2.6, RCP4.5, RCP6.0 and RCP8.5 scenarios respectively from 2060 to 2080. The predicted amounts of fertile soil loss from agricultural land in a year were predicted to be 55.5 million tonnes at present, and 62.7, 59.9, 61.7 and 58.1 under RCP2.6, RCP4.5, RCP6.0 and RCP8.5 respectively. This confirms that approximately 30% of the total erosion occurs over the agricultural lands. In this respect, degraded forests, scrub and arable lands were subjected to the highest erosion rate (68%) of the total, whereas, fruit trees and berry plantations reflected the lowest erosion rates. Low soil organic carbon, sparse vegetation cover and variable climatic conditions significantly enhanced the erosion of the cultivated lands by primarily removing the potential food for organisms. Finally, process-based models offer a valuable resource for decision-makers when improving environmental management schemes and also decrease uncertainty when considering risks.

Keywords Erosion · Climate change scenarios · Land use · Turkey · PESERA

S. Berberoglu · A. Cilek (✉) · C. Donmez
Faculty of Architecture, Landscape Architecture Department, Cukurova University, 01330 Adana, Turkey
e-mail: acilek@cu.edu.tr

M. Kirkby · B. Irvine
School of Geography, University of Leeds, Leeds, UK

Introduction

Recently, soil erosion has been a global ecological concern exposing significant threats to the environment and the people. This disaster is induced by human activities and climate change in arid, semi-arid and semi-humid areas causing soil nutrient loss and land degradation. Further, soil erosion also exacerbates the extent of already existing land-related issues such as drought, floods, landslides and other disasters (Munodawafa 2007; Rickson 2014; Arnhold et al. 2014; Zeng et al. 2017). Soil erosion by water (WSE) has become a pertinent global problem by the continuous reduction of the natural resources coupled with the impacts of climate change. Furthermore, soils are more susceptible to erosion for various reasons, which include construction activities, forest fires, deforestation, inappropriate agricultural practices and overgrazing. WSE is a severe long-term concern, affecting all countries in Europe in varying magnitudes. The countries in Mediterranean Europe are susceptible to erosion, mainly due to prolonged dry phases and dense erosive rains dropping onto steep slopes that are characterised by breakable soil aggregates (Terranova et al. 2009).

Soil erosion thus poses as a different environmental and social problem intervening with human survival and hindering the global socio-economic sustainable development (Han et al. 2016). Erosion stands as a major soil threat within the eight listed in the Soil Thematic Strategy of the European Commission. The vast majority of land in the world has been exposed to soil erosion, causing a dramatic decrease in crop productivity, agricultural yield and income (Wuepper et al. 2020; Begum Nasir Ahmad et al. 2020; Uzuner and Dengiz 2020). It washes away nutrients and transports pesticides and other harmful farm chemicals into the streams and groundwater resources (Gallaher and Hawf 1997; Vieira et al. 2018). Throughout the twentieth-century, soil erosion increased (Angima et al. 2003; Li et al. 2017) and has become such a severe environmental challenge that it can now be deemed a crisis (Trimble 2000; Fernández and Vega 2016).

Climate change, desertification, land degradation and drought are amongst the most critical issues as they affect over 4 billion hectares of land in more than 164 countries and directly impact approximately 1.5 billion people. These hazards threaten not only the environment but also the economy, food security and social life in Turkey and a similar part of the globe.

In the previous years, soil scientists have advocated their significant concerns on climate change and its impacts on the present and possible future changes upon soils. Altered precipitation regimes owing to the dynamicity of the climate, undoubtedly have enhanced the risk for soil erosion, surface runoff and related environmental consequences. A large variation in terms of regional, seasonal and temporal aspects have been noted in the precipitation for both simulated climate regimes and current climate records. The vulnerability response to soil erosion and runoff varies for the different types of landscapes. The Intergovernmental Panel on Climate Change (IPCC) stated that in the past century, there had been an increase in surface temperature worldwide. This has happened in two distinct phases, namely within the 1910s and 1940s (0.35 °C) and more intensely within the 1970s and recently (0.55 °C) (IPCC Climate Change 2007). In the Coupled Model Intercomparison Project Phase 5 (CMIP5), future climate data were obtained in conjunction to the RCP (Representative Concentration Pathways) settings (Taylor et al. 2012). Four RCP settings were chosen with recommended CO_2 concentrations attaining 421 ppm (RCP2.6), 538 ppm (RCP4.5), 670 ppm (RCP6.0) and 936 ppm (RCP 8.5) by the year 2100. Each RCP scenario describes a particular discharge trail and consequent radioactive forcing. The future climate data were derived in conjunction with these settings (Nazarenko et al. 2015).

Planners and decision-makers use large-scale modelling to develop appropriate land management strategies. Up to now, research in soil erosion on a large scale has used two common methodologies: (1) assessing soil loss by extrapolating from the plot and micro-catchment scales to regional, catchment and watershed scales (Zobeck et al. 2000; Brazier et al. 2001; Zhang et al. 2002; Renschler and Harbor 2002; Yang et al. 2003; Li et al. 2017; Amanambu et al. 2019) and (2) assessing the present models or the regional erosion issues (Le Bissonnais et al. 2002; Wang et al. 2003; Finlayson and Montgomery 2003; Beskow et al. 2009; Vinet and Zhedanov 2011; Panagos et al. 2013, 2014; Ochoa et al. 2016). These two methodologies both hit the significant stumbling block of spatial heterogeneity at larger scales and have shown the requirement of applying additional techniques for many regions (Fu et al. 2005).

The consequences of environmental change have been a major concern owing to their impact on the natural resources and landscapes. In this regard, modelling plays a supporting role by allowing to fathom environment and reporting of the likely outcomes of environmental change (Unal and Uslu 2018; Unal et al. 2018). Soil erosion modelling is used for the planning of transformation programs to predict residue input into recently planned reservoirs, to assist in the selection of soil conservation strategies and to gain an understanding of the occurring processes. Nearing et al. (2005) stated that if the time or cost involved in taking soil erosion measurements is excessive, then models are to be used. Much effort has been put into predicting soil loss and understanding the mechanisms of soil erosion via many process-based or empirical simulations that have been developed globally (Russell and William 2001; Merritt et al. 2003). Empirical, conceptual and physically based models are the three broad categories of soil erosion models. Field observations and standard runoff on uniform slopes serve as the basis for empirical models. The application of such models is limited to various areas. However, the development of the model database requires appropriate adaptation to the new environment which is both time and capital intensive. Thus, in order to collect a set of data large enough to calibrate over equations, the authors used a physically based model to produce the synthetic data enabling to reduce the investment of resources and time needed for such a calibration. Conceptual models simulate the processes of WSE by observed associations amongst the involved variables. Physically based models attempt to partially replace empirical relationships with mathematical expressions based on scientific and experimental principles. Efforts are currently being put into physical models because they are the substitutes for conceptual and alternative modelling. Some significant physical models include EuroSEM (European Soil Erosion Model) (Morgan et al. 1990); SHE–SED (Wicks and Bathurst 1996) which is an incorporated component of the 'Système Hydrologique Européen' (Abbott et al. 1986), ANSWERS (Areal Nonpoint Source Watershed Environment Response Simulation) (Beasley et al. 1980), PESERA (Pan-European Soil Erosion Risk Assessment) (Gobin et al. 2003; Kirkby et al. 2003) and WEPP (Water Erosion Prediction Project) (Nearing et al. 1989).

The amount and supply of water for human consumption and agriculture is a significant constraint for Turkey which directly or indirectly influences the quality of life. In the twenty-first century, inappropriate land use and climate changes will tend to increase soil erosion and degradation. New challenges may arise as specific soil thresholds are surpassed due to the numerous adverse effects of the currently augmented soil erosion (Boardman and Favis-Mortlock 2001). Erosion and climate are, therefore, co-dependent elements in our environment and the hydrologic cycle of the Earth. Turkey is particularly vulnerable to erosion due to its geographic position, climate, topography and soil conditions. Therefore, the spatial and temporal monitoring of soil erosion in Turkey is of great importance and necessitates a plan for land management decisions. This study aims (i) to evaluate the impact of land use/cover on soil erosion rates for each watershed, (ii) to validate sediment export measurement derived from gauging stations with the ability of the PESERA model and (iii) to compare the spatial patterns of soil erosion rates for land use/cover under climate change scenarios. This study will provide a basis for a comparison of the soil erosion sensitivity in Turkey under climate change.

Materials and method

Study area

Turkey is located in the northern hemisphere between the 36°–42° northern longitudes and the 26°–45° eastern latitudes and has an area of 783,562 km^2. The country is located where Europe runs into Asia, making a connection between these two continents. The Asian part is known as Anatolia and is separated by the Dardanelles, the Sea of Marmara and the Bosporus. The European part is known as Thrace (Fig. 1).

Turkey has a wealth of diverse land use/land cover types, climate zones, soil and topography. The country is prone to erosion at different levels because of degrading land use and topography. Agricultural lands in Turkey make up to 40% of the total, whereas the pasture and rangelands, the forests and the remaining settlements are 26%, 28% and 6%, respectively according to the CORINE land-use data. The dominant arable crops are mainly wheat, sugar beet, barley, potatoes, maize, soybeans, rice, sunflower and soybeans. The Ministry of Forestry and Water Affairs records document that forests occupy 21.2 million ha of land where half of the forestlands are productive and the remainder is degraded. About 53% of the forestlands consist of broad-leaved species, with 42% of conifers and 5% of mixed and broad-leaved trees.

Several climate zones exist in the country due to its geographical location and topography. Turkey has different climatic regions, ranging from the Mediterranean to semi-arid and arid; this is because of its exceptional geographical position at the transitional zone between Asia and Europe (Cilek et al. 2020; Akça et al. 2020). The soils differ in close proximities and are highly variable reflecting the diverse topography and geologic past. Thus, the vulnerability to degradation of the soils

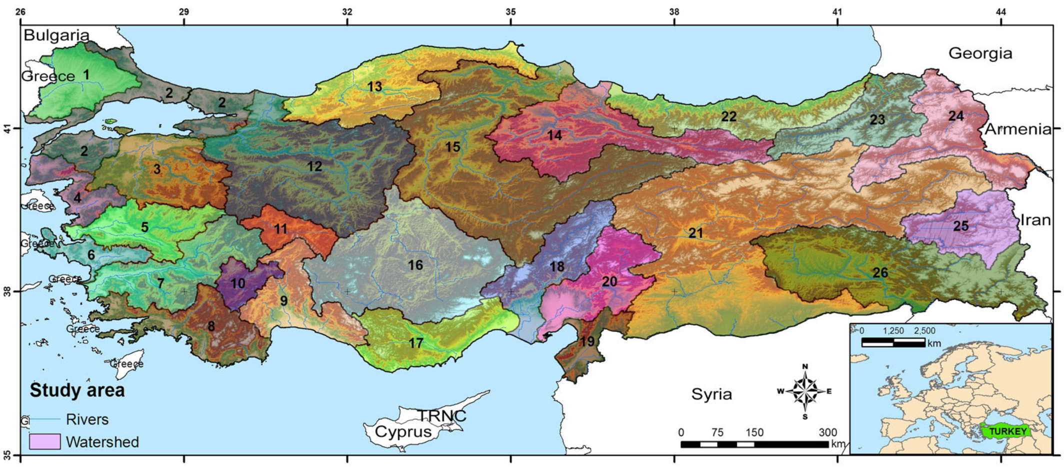

Fig. 1 Location of the study area

of the semi-arid regions of Turkey may stem from the poor ability to resist erosion due to the undulating and/or sloping topography coupled by their degraded physical and chemical properties. In this context, the highly eroded very shallow to shallow soils (67.7% of the total area) are distributed mainly on the surfaces of the very steep slopes (47.5% of the very shallow to shallow soils), whereas only a small increment of the soils are located on the flatlands (12.8%) of the country and about only a 14.2% of the land area is covered by deep soils The dominant textural classes of the soils of Turkey vary from loamy (50.49%) to clayey loam (41.44%) and are derived from the mixed materials transported from diverse topographies and climatic regions. Salinity and erosion are the two primary factors that hinder the fertility of Turkish soils. The man-induced secondary soil salinity is widely distributed in the irrigated parts of central, western and south-eastern Turkey. The most widely distributed soils are Fluvisols (11.36%), Luvisols (5.87%), Cambisols (67.56%), Kastanozems (6.89%) and others (8.32%) as shown in Table 1.

Methodology

The research objectives of this study were to estimate the soil erosion rates under four different climate change scenarios for various land use/cover types and to analyse the spatial extent of the climate change impact. The study includes three steps of analyses including (i) modelling of the present soil erosion on a watershed basis using the PESERA model, (ii) analysis of the accuracy of the model efficiency with gauging station data and (iii) the temporal and spatial changes in soil erosion under climate change scenarios.

Pan-European Soil Erosion Risk Assessment (PESERA) model

The PESERA model was built for large-area applications, and based on producing explanations concerning rill erosion and physical processes controlling sheet

Table 1 Distribution of the soil groups in Turkey

FAO soil name	FAO85_ID	Total area (ha)	Percentage of Turkey's area (%)
Cambisol	B	162,955,669	20.80
Calcaric Cambisol	Ba	294,914,683	37.64
Calcaro-Chromic Cambisol	Bcc	23,085,626	2.95
Vertic Cambisol	Bv	48,376,522	6.17
Calci-Vertic Cambisol	Bvk	36,958,295	4.72
Redzina	E	7,623,024	0.97
Calcaric Fluvisol	Jc	33,402,565	4.26
Fluvi-Calcaric Fluvisol	Jcf	55,132,590	7.04
Fluvi-Eutric Fluvisol	Jef	498,978	0.06
Haplic Kastanozem	Kh	53,980,419	6.89
Albic Luvisol	La	28,184,227	3.60
Chromic Luvisol	Lc	17,799,118	2.27
Histosol	O	274,441	0.04
Arenesol	Q	289,720	0.04
Calcaric Regosol	Rc	6,915,962	0.88
Calcaro-Chromic Vertisol	Vcc	13,170,162	1.68
Total		783,562,000	100

erosion. However, it is intended to keep the process simple enough to keep the implementation capability high using the data at the European scale.

An indicator of soil erosion risk at the regional scale was published by Kirkby et al. (2008). The PESERA model is centred around a one-dimensional hydrological balance that partitions precipitation between evapotranspiration, overland flow, subsurface flow and groundwater recharge. It differs from the SVAT (Soil-Vegetation-Atmosphere Transfer) scheme by focussing on water and sidestepping energy balance considerations by using potential evapotranspiration as an input variable. Infiltration-excess overland flow is estimated from a near-surface soil water storage capacity and the frequency distribution of daily rainfalls, and, together with relief and soil type, drives the soil erosion estimate. An integrated plant growth model, dependent on actual evapotranspiration, drives a biomass model for vegetation and soil organic matter, and, in turn, the vegetation cover and organic matter dynamically control the soil water storage capacity, which generally varies both seasonally and from year to year. Sediment transport and soil erosion predicted with PESERA estimate the prevailing rill and sheet erosion processes (Kirkby et al. 2003). The model estimates the erosion rate, rainfall interception by plants, water storage and terrestrial humus and vegetation biomass for each month and per annum independently (Kirkby and Neale 1987; Kirkby and Cox 1995; Kirkby et al. 2000).

PESERA as a spatially distributed physically based soil erosion model was developed to estimate soil erosion for the whole of Europe at a spatial resolution of 1 km. It has been designed to produce state-of-the-art soil risk evaluation at a European scale, and, compared with other models, it produces an additional estimate of WSE for the whole of Europe (Kirkby et al. 2000, 2003, 2004). Soil erosion estimated by PESERA is conveyed as the amount of sediment carried to the base of a hillside land delivered to the channel network. Channel erosion, channel routing, permanent gullies and channel delivery processes are thus not estimated (Kirkby et al. 2004). The model combines the impacts of soil, climate, vegetation and topography and soil erosion (E; t ha^{-1} yr^{-1}) in the PESERA model is determined by:

$$E = k \Delta \Omega \quad (1)$$

where k represents erodibility based on vegetation cover, soil parameters and land use, Δ represents the prospective topography based on a digital elevation model (DEM) and Ω represents the prospective vegetation/climate and runoff soil erosion based on a plant growth model, vegetation cover and gridded climate data (Fig. 2) (Kirkby et al. 2008).

The major watershed of Turkey was classified to fit the model. The model was calibrated against data from erosion plots. The whole slope is represented by a raster model with a single cell. It can simulate climate change and land use as it indicates a vegetation growth routine based on changing vegetation cover in response to specific climatic conditions. Similarly, this model determines the average long-term erosion per month for a whole year (Kirkby et al. 2003). The protective effects of vegetation from soil erosion are many and may vary depending upon the surrounding conditions. Some of the significant effects of vegetation in terms of averting soil erosion are as follows; firstly, vegetation renders a shielding effect to the soil from the impact of rain splash and crusting; secondly, it intercepts rainfall that is lost to evaporation; and lastly, it enhances the short-term dynamic storage and release of soil moisture by enriching the soil with organic matter. The ultimate aim of either of the effects is to increase the runoff threshold. Additional impacts of vegetation may include the implications in terms of soil roughness. Enhanced soil roughness not only reduces the overland flow velocity but also increases soil erodibility by binding the soil with shallow root mats, to be specific grasses.

Considering the climatic aspect of soil erosion, an appropriate sum up of the frequency distribution of storm rainfalls is required. The same would give rise to the rationale for combining the effects of topography, soils and climate into a single integrated erosion forecast. In the case of erosion, both low- and high-frequency components of the climate hold immense importance. Generating overland flow mainly depends on the high-frequency rainfall (Kirkby et al. 2003).

Precipitation is divided into saturation excess runoff, evapotranspiration, snowmelt, change in soil moisture storage and infiltration-excess runoff. Infiltration-excess overland flow depends on the verge runoff obtained from the vegetation cover, organic matter and soil characteristics. The conversion of daily rainfall to daily overall overland slow runoff is performed using a simple storage threshold model.

It is presumed that the sediments present at the base of the hill mainly is a result of soil erodibility and a combined outcome of runoff slope gradient and release.

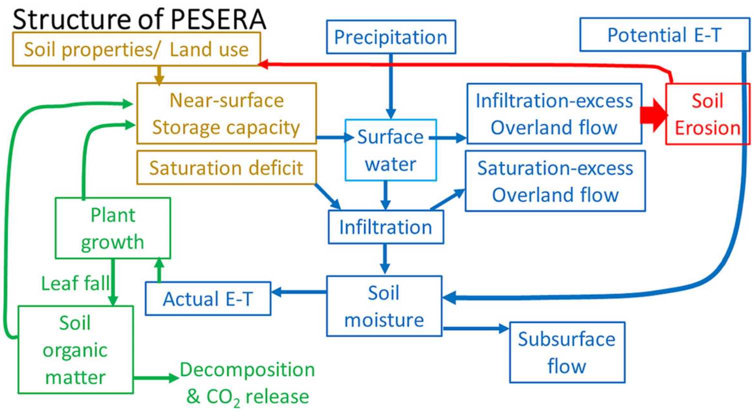

Fig. 2 PESERA modelling scheme

Soil texture is closely related to erodibility, and the value is highest for fine sand and silt soils with low clay content. However, in terms of vegetation and Soil Organic Matter (SOM), erodibility responds significantly. For vegetation, the stem is responsible for rendering roughness which in turn reduces flow velocity and the impact of flow on the soil. The effects of SOM and clay content is realised through the increase in the size of stable soil aggregates (Kirkby et al. 2004).

The PESERA model can be implemented in two modes, including an estimate of sediment yield data and a distributed estimate of erosion risk, by operating on grid data. Overall, 128 input data layers derived from a large dataset covers land use, soil characteristics, climate, crop type, topography and planting dates (Fig. 3 and Table 2).

Data

The different factors that significantly influence erosion are climate, land use/cover, soil properties and topography (Fig. 3). Despite the factors being itself complex, the degree of complexity is further raised by the interaction between the factors. A scientific rationale is highly essential in the course of creating synthetic indicators. The rationale can be achieved by combining the abovementioned factors into composite indicators. In this regard, PESERA, the functioning of which is based upon physical parameters holds promise.

Climate variables were interpolated with a grid size of 250 m using 950 climate stations of Turkish State Metrological Service (TSMS 2012). Rainfall depth, number of rainy days, average rain in a day and its standard deviation were derived from daily rainfall depths data (Fig. 4). Additional climate-related variables were possible evapotranspiration, daily temperature range and average monthly temperature values.

The soil input variables for PESERA were derived from the Soils Database of Turkey at 1: 25000 scales through pedotransfer rules (PTRs). The soil variables comprised soil water storage, soil surface properties (crust storage), scale depth, erodibility and soil moisture. Crusting and erodibility, resulting in five classes per parameter, were derived using PTRs from soil texture classes and soil types. A chained pedo-transfer rule was implemented to derive the soil erodibility parameters from soil classes (third level FAO legend), dominant soils, secondary surface textural and parent material classes (third level). Information pertaining to the soil such as the positive or negative effect of organic matter, carbonates, cations and other pedo-genetic characteristics led to the development of five classes of a physico-chemical parameter. The different principles that guide the pedo-transfer rule for determining the physico-chemical soil property are (i) very favourable: 'Histosols'; ii) very unfavourable: 'Solonchak', 'Solonetz'; iii) favourable: Rendzina', 'Chernozem', 'Kastanozem', 'Greyzem', 'Phaeozem' and 'Ferralsol'; iv) unfavourable: 'Podzoluvisol', 'Podzol', 'Arenosol', 'Andosol', 'Planosol', 'Xerosol'; v) medium: 'Acrisol', 'Lithosol', 'Fluvisol', 'Regosol', 'Ranker', 'Vertisol', and all other except unfavourable if: 'dystric', 'gleyic', 'albic', 'planic', 'spodic', and favourable if: 'calcaric', 'chromic', 'calcic', 'humic'. A function of dominant soil surface texture, the secondary soil surface texture and the type of parent material is the crusting textural/parent material parameter. The low crusting susceptibility class comprises the texture classes of coarse, very fine and fine. The medium or high crusting susceptibility class, on the contrary, involves the fine and medium textures

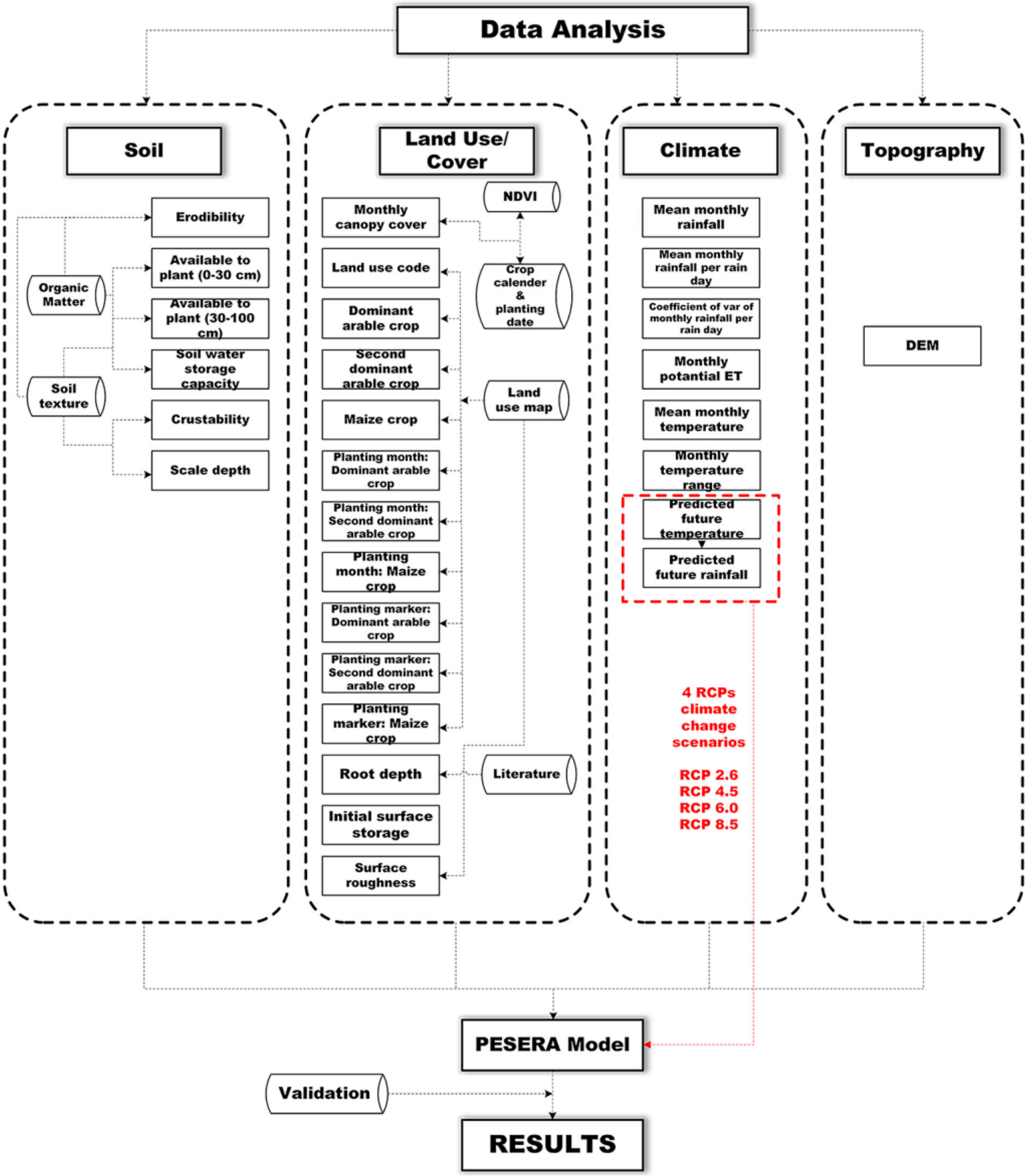

Fig. 3 Flowchart of methodology and procedures (Cilek 2017)

but distinct demarcation depends upon the secondary texture class and the parent material type. A combination of the dominant soil surface texture and the parent material type influences erodibility via the textural/parent material parameter. The low erodibility category involves massive rocks such as granite or limestone. On the other hand, loose rocks like sand or molasses fall under the high erodibility category. Soil water storage is

Table 2 Input variables for the PESERA model developed by (Cilek 2017; Kirkby et al. 2003)

Input variables	Range	Units	Source	Explanation
Climate				
Mean monthly rainfall	0–130	mm	Meteorological data from Turkish State Meteorological Service (1975–2011)	Interpolated using thin-plate smoothing splines
Mean monthly rainfall per rain day	0–50	mm		
Coefficient of variation of monthly rainfall per rain day	1–10	–		
Mean monthly temperature	−21.4-37.3	°C		
Mean monthly temperature range	2.4–18.4	°C		
Mean monthly potential evapotranspiration	0–300	mm		
Soil				
Soil water available to plant (0–30 cm)	0–90	mm	Soils Database of Turkey	Soil parameters arederived from texture and physical-chemical data from pedotransferrules
Soil water available to plant (30–100 cm)	0–154	mm		
Soil water storage capacity (this is the maximum capacity of soil before runoff)	0–205	mm		
Profile depth of soil textures		–		
Crusting	5–30	–		
Erodibility	1–5	–		
	1–5			
Land use/cover				
Arable crop, planting month, planting marker	–	–	Sage University of Wisconsin Crop Calendar Database, CORINE	Arable crop, cereal planting dates, generalized from the Sage University of Wisconsin Crop Calendar Database, CORINE
Land use/cover	–	–		
Root depth	10–1000	mm		
Initial surface storage	0–10	–		
Surface roughness reduction per month	0.50	%		
Monthly canopy cover	0–100	%		
Topography				
Standard deviation of elevation in 750 m radius	–	m	Gtopo30 DEM	30 m global ASTER DEM

described by three different measures as PTRs enable to create soil data currently unavailable with a spatial resolution of 250 m across Turkey (Fig. 5). The soil hydrological characteristics were extracted from the soil databases of Turkey from the General Directorate of Agricultural Reform (TRGM) at a 250 m grid size. The variables needed for the crop growth model and ground cover were approximated from the CORINE land cover data (CLC 2012) at a resolution of 250 m and used in conjunction with cereal planting dates.

CORINE land cover data was introduced to PESERA at a 250-m spatial resolution (Fig. 6). The mapping scale of this classification was 1:100000 and mapping accuracy is at least 100 m. The minimum mapping unit was 25 ha and a minimum width of units was 100 m. The Crop Calendar Database from the Center for Sustainability and the Global Environment (SAGE) at the University of Wisconsin-Madison was used within the growth models for a natural crop or parameters for crops (Sacks et al. 2010). Cereal planting dates were combined with the land-use data, and the Crop Calendar Database was used to derive the tillage, harvest and average planting dates.

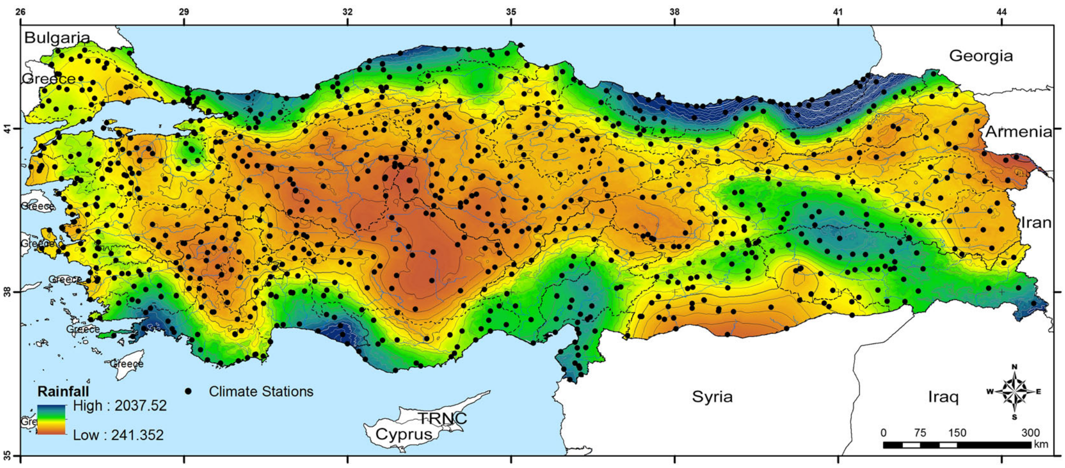

Fig. 4 Climate stations and annual rainfall map for Turkey, 1975–2012

The GTOPO30 Digital Elevation Model at a spatial resolution of 30 m derived from Aster Satellite sensor data was used to include topographical dynamics for the erosion modelling within PESERA (Fig. 7). The local relief is the input variable required by the model and this was estimated using the DEM as the standard deviation of DEM elevations within a 750-m diameter circle around every cell.

Climate change scenarios for soil erosion modelling

Climate model simulation, which corresponds to global scenarios, is based on global climate models developed by modelling groups around the world through CMIP5 (Coupled Model Intercomparison Project Phase 5), which supports the 5th IPCC report. The CMIP5 was used as the climate projection for Turkey for the period from 2060 to 2100 in this study. RCP scenarios introduced at the IPCC 5th Assessment Report utilised at the HadGEM2-AO Global Circulation Model (GCM) of the CMIP5 project were used for Turkey. The model was run for a reference time during 1960 to 2000 and for a future period with a spatial resolution of 1 km from the WorldClim research group. These are the latest climate projections from the GCMs that were used in the IPCC's 5th Assessment Report. The GCM yield was adjusted (bias-corrected) and rationalised as the standard 'current' climate (Hijmans et al. 2005). The General linear model using bioclimatic factors (dependent variables) and covariates (independent variables) was utilised to downscale the available data from 1 km to 250 m spatial resolution. The post creation of the linear regression model and the generalisation of the mathematical model was done for the geographical space, and the

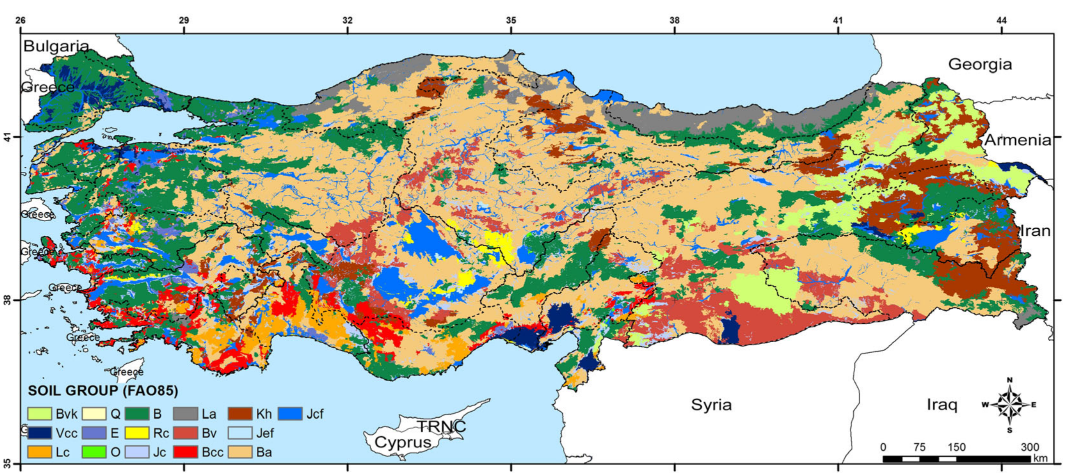

Fig. 5 Soil map of Turkey (According to FAO 85 Soil Classification)

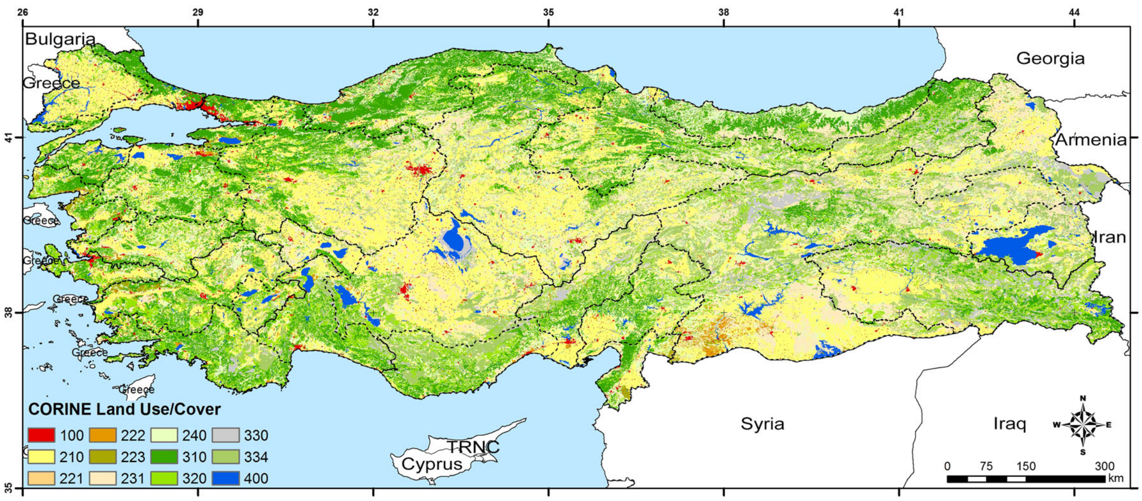

Fig. 6 CORINE land cover map of Turkey (100: artificial land; 210: arable land; 221: vineyards; 222: fruit trees and berry plantations; 223: olive groves; 231: pastures and grassland; 240: heterogeneous agricultural land; 310: forests; 320: scrubland; 330: bare rocks; 334: degraded forests; 400: water surfaces and wetland)

downscaling of the bioclimatic variables was performed to 250 m pixel size utilising the 250 m resolution covariate maps.

Results

The PESERA erosion model was configurated for the whole country. Turkey's climate change scenarios were introduced at a spatial resolution of 250 m to evaluate the effects of global climate change on soil erosion. Climate change scenarios of four RCPs from the 5th IPCC Assessment Report, including RCP 2.6 to 8.5 until the year 2070 were with PESERA. According to the climate change scenarios, Turkey will suffer a temperature increase of up to 1.4 ± 0.7 °C and a rainfall decrease of 30 ± 11 mm until the year 2070. The sparse vegetation cover will intensify the impact of rainfall, and there will be an actual increase in evapotranspiration due to the temperature increase.

Evaluation of annual soil loss in Turkey

The results of this study showed the amount of the temporal and spatial distribution of erosion in t ha^{-1} yr^{-1}. Approximately 287.5 million tonnes of soil

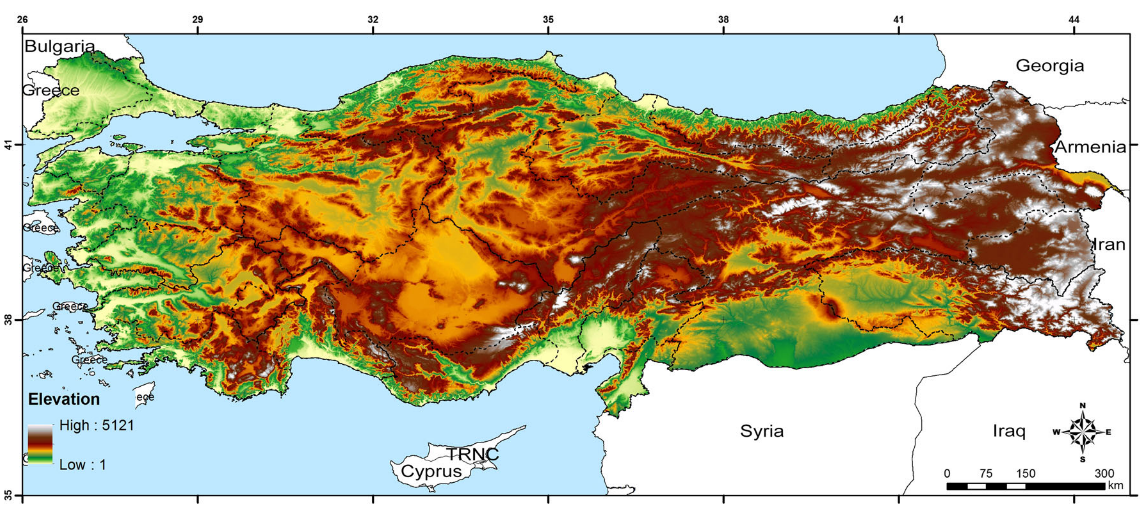

Fig. 7 Digital elevation model of Turkey derived from ASTER Data

have been lost in 1 year. The estimated soil loss ranged from 0 to 1087 t yr^{-1} and the average soil loss was 3.88 t ha^{-1} yr^{-1} with a standard deviation of 15.08, according to the model outcomes. The Aras Basin (24) was the least, whereas the Tigris Basin (26) was the most prone ones to erosion. The Tigris Basin experiences a significant amount of soil erosion due to its variable topography, heavy rainfall and large values of erodibility. In addition, naturally degraded regions are considered to be amongst the factors contributing to this erosion (Table 3).

Once the overall amount was assessed as a definite variable, it was determined that 1.86% of the study area never experienced any erosion (except wetlands, water surfaces and bare rock), 46.32% faced erosion from 0 to 0.5 t ha^{-1} yr^{-1} and 14.40% of the region faced erosion from 0.5 to 1 t ha^{-1} yr^{-1} (Table 4). In total, these regions cover 62.57% of the land area of Turkey (Fig. 8).

Forests, pastures and grasslands are the regions with the lowest risk of erosion, whereas degraded natural vegetation and scrublands are the regions at the highest risk of erosion according to the PESERA results. Water surfaces, bare lands and wetlands determined the quantity of any erosion (Table 5). This evidently depicts that 19% of the overall erosion occurs over arable lands, 69% occurs over the degraded forest regions, and scrublands and 2% of the remaining portion is from urban and forest lands.

Table 3 Model outcomes of soil erosion for each river basin in Turkey

River basin in Turkey	Basin area (ha)	Annual erosion				Std	Percentage sum of erosion (%)
		Min (t ha^{-1} yr^{-1})	Max	Mean	Total (t yr^{-1})		
(01) Meriç Ergene river basin	1,446,560	0	65.8	1.24	1,671,588	2.8	0.59
(02) Marmara river basin	1,686,190	0	117.8	1.85	3,976,831	5.0	1.39
(03) Susurluk river basin	2,429,150	0	109.3	1.74	4,150,856	4.5	1.45
(04) North Aegean river basin	988,287	0	133.1	2.38	2,306,900	6.4	0.81
(05) Gediz river basin	1,715,540	0	132.9	2.08	3,512,219	5.2	1.23
(06) Kucuk Menderes river basin	697,435	0	147.8	1.72	1,164,088	4.6	0.41
(07) Buyuk Menderes river basin	2,602,000	0	265.8	3.04	7,785,238	8.1	2.73
(08) West Mediterranean river basin	2,100,680	0	540.3	5.27	10,371,044	16.4	3.63
(09) Antalya river basin	1,953,360	0	702.9	7.94	14,281,819	23.7	5
(10) Burdur river basin	647,022	0	86.0	1.85	1,083,313	3.2	0.38
(11) Akarcay river basin	799,542	0	61.1	1.36	1,022,644	2.5	0.36
(12) Sakarya river basin	5,892,650	0	331.5	1.58	9,223,881	4.3	3.23
(13) West Black Sea river basin	2,887,070	0	256.3	2.61	7,422,169	9.1	2.6
(14) Yesilirmak river basin	3,861,560	0	111.3	2.17	8,184,813	5.3	2.87
(15) Kizilirmak river basin	8,223,410	0	172.3	1.63	12,996,750	4.0	4.55
(16) Konya closed river basin	5,437,010	0	232.3	1.31	6,476,344	3.7	2.27
(17) East Mediterranean river basin	2,235,730	0	447.8	11.1	24,071,625	24.2	8.43
(18) Seyhan river basin	2,168,070	0	313.9	3.93	7,963,844	12.3	2.79
(19) Asi river basin	783,898	0	316.2	8.84	6,718,738	22.9	2.35
(20) Ceyhan river basin	2,147,080	0	549.6	6.88	14,331,275	18.9	5.02
(21) Euphrates river basin	12,182,200	0	444.0	2.92	32,867,313	9.2	11.51
(22) East Black Sea river basin	2,382,610	0	524.6	3.07	7,148,294	7.1	2.5
(23) Coruh river basin	2,023,900	0	402.3	3.72	7,131,250	11.8	2.5
(24) Aras river basin	2,792,860	0	63.8	0.57	1,453,394	0.9	0.51
(25) Van lake river basin	1,797,260	0	492.7	2.03	2,702,225	7.5	0.95
(26) Tigris river basin	5,423,800	0	1086.6	17.6	85,413,563	43.3	29.92
Turkey	77,304,874	0	1086.6	3.88	285,432,013	15.08	100

Table 4 Categorised model results of soil erosion

Erosion amounts (t ha^{-1} yr^{-1})	Area (ha)	Annual erosion		Standard deviation	Percentange sum of erosion
		Mean (t ha^{-1} yr^{-1})	Total (t yr^{-1})		
0	1,364,540	0.00	0	0.00	1.86
0–0.5	34,038,900	0.25	8,463,437	0.11	46.32
0.5–1	10,580,700	0.72	7,593,562	0.14	14.40
1–2	9,401,410	1.43	13,417,437	0.28	12.79
2–5	8,787,790	3.15	27,698,562	0.84	11.96
5–10	3,938,870	7.00	27,582,437	1.41	5.36
10–20	2,442,430	14.07	34,361,625	2.83	3.32
20–50	1,852,160	31.19	57,767,937	8.36	2.52
> 50	1,081,844	100.39	108,605,974	61.94	1.47

Distributions of monthly soil erosion

There was an increase in the monthly erosion estimated during the autumn season from August to January, due to high runoff and heavy rain (Fig. 9). Nonetheless, there was a severe decline in erosion during the winter season when the rainfall turned to snow (Fig. 10). The least amount of erosion was estimated for June, whereas the highest amount was estimated for December (Table 6).

Model validation using sediment measurement in streams

Model validation was implemented using the sediment records of 107 gauging stations from various river basins. These sedimentation records were calculated by the General Directorate of the Electric Power Research Survey and Development Administration (EIE) of the State Hydraulics Works (DSI) using bathymetric surveys. Twenty-six basins were portrayed using ASTER DEM with a resolution of 30 m. Stream networks were used to determine the sub-catchments to locate gauging stations, lakes and dams (Fig. 11).

The monthly average sediment measurements were derived from the 105 river gauging stations for the period from 2005 to 2012. Each gauging station records indicated the quantity of the sediment running from its upper sub-catchment. The relationship between the simulated and measured data on the upper sub-catchment sediment and the PESERA erosion model was reviewed. The calibrated Pearson correlation (r) was determined as 93.9% (Fig. 12). These measured sediment data from 105 gauging stations provided some partial validation for the estimates from the PESERA model but should be treated with caution since the

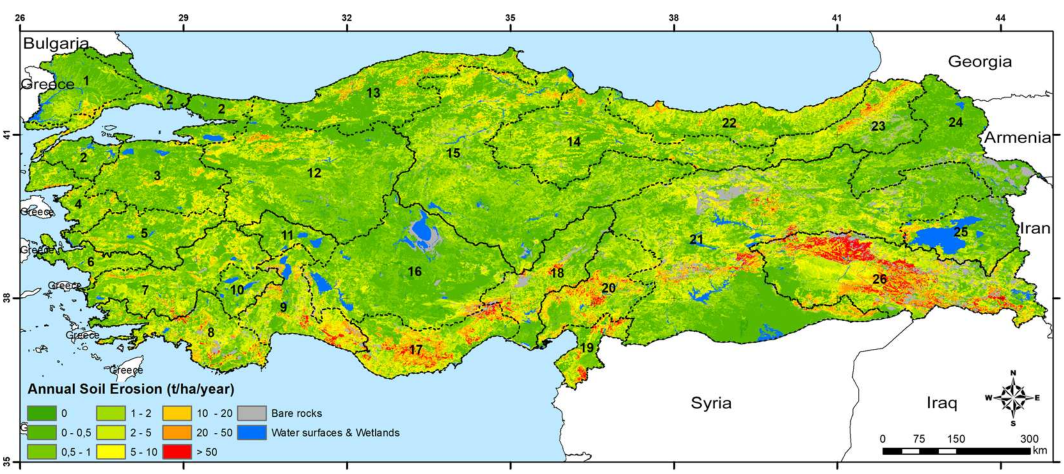

Fig. 8 Map of estimated soil erosion in Turkey

Table 5 Model results of PESERA land cover

PESERA code	Description	Area (ha)	Mean (t ha^{-} yr^{-1})	STD	Total (t yr^{-1})	Percentage sum of erosion (%)
100	Artificial land	1,199,460	0.99	3.13	1,187,969	0.42
210	Arable land	17,807,600	3.12	8.14	55,472,688	19.43
221	Vineyards	267,594	5.9	14.66	1,578,919	0.55
222	Fruit trees and berry plantations	405,713	3.06	8.68	1,241,663	0.43
223	Olive groves	362,650	10.06	18.33	3,648,850	1.28
231	Pastures and grassland	10,418,500	0.25	1.01	2,655,225	0.93
240	Heterogeneous agricultural land	12,331,600	1.58	5.2	19,505,563	6.83
310	Forest	12,112,700	0.29	0.73	3,556,431	1.25
320	Scrub	8,355,550	11.36	27.29	94,921,875	33.25
330	Bare land	2,321,831	0	0	0	0.00
334	Degraded forests	10,227,400	9.95	27.06	101,721,250	35.63
400	Water surfaces and wetland	1,785,950	0	0	0	0.00

model estimates sediment entering the fluvial system and gauging station data measures sediment leaving the system and consequently, the possible flood plain sediment storage is not taken into account.

The response of soil erosion to climate change

Regarding the climate time-series, the PESERA model was run over a simulated 20-year period (2060–2080). The model simulations revealed a yearly and monthly inconsistency in the response of soil erosion to the various climate change scenarios introduced by the IPCC. Therefore, the simulations of future erosion were based on four climate change scenarios, including the RCP 2.6, RCP 4.5, RCP 6.0 and RCP 8.5 in turn revealing the significant fluctuations of the long-term mean quantities of air temperature and rainfall (Fig. 13).

There is a strong agreement between the current situation of Turkey and the four scenarios regarding the rate of soil erosion (Table 7). Figure 14 illustrates the change in the erosion rate from the current situation to the end of the twenty-first century, considering the climate change scenarios. The modelling outcomes pointed out to the possible large upsurge in the erosion rates, particularly in the south-eastern and Mediterranean regions of Turkey under climate change scenarios.

Climate change has direct and indirect impacts on soil erosion. The changes in the amount of rainfall, rainfall intensity and rainfall spatio-temporal distribution directly affect soil erosion, while increasing temperature, anthropogenic and socio-economic factors have indirect effects. In this context, the increasing amount of rainfall leads to higher erosivity by accelerating surface runoff. The temperature mainly affects plant biomass, amount of evapotranspiration, canopy cover, soil moisture and snow, while both rainfall and temperature factors could change the soil erosion rate positively or negatively by changing agricultural crop management. As per the indications from the IPCC scenarios, it can be stated that climate change has a significant impact on Turkey. Conversely, it can also be said that the region where Turkey is located is highly vulnerable to climate change impacts based on the analysis and indications of the IPCC scenarios. The shift of the storm towards the northern direction is expected to result in higher precipitation in the north and lower precipitation in the southern parts of Turkey. These predicted changes in precipitation are expected to affect surface runoff and subsequent soil erosion mechanisms. This effect does not always have adverse effects on soil erosion. It is possible to reduce surface runoff and soil erosion by increasing the biomass and canopy cover of plants with more precipitation. With the increasing atmospheric CO_2 concentration and temperature, the plant biomass production and evapotranspiration rate increases, soil moisture decreases, and in turn surface runoff and soil erosion decrease with the increasing soil percolation capacity. However, the effects of high CO_2 concentration on soil erosion are not always positive, especially in areas with high slopes and elevation. In this respect, plant

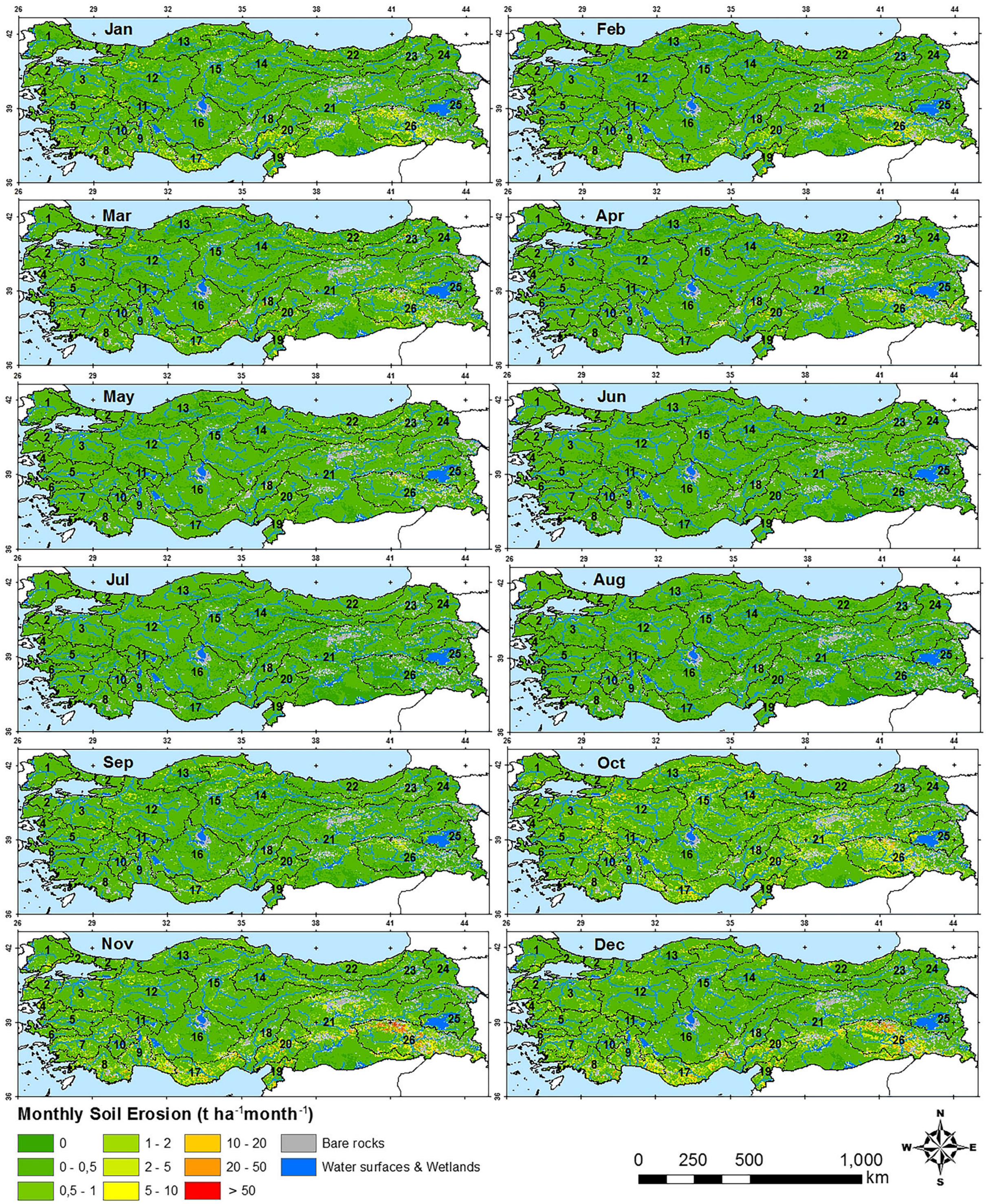

Fig. 9 Maps of estimated monthly soil erosion of Turkey

growth may also decrease in turn increasing snow-melt due to extreme temperature stresses. This will increase sediment transport during the period when the snow starts to melt together with an intense

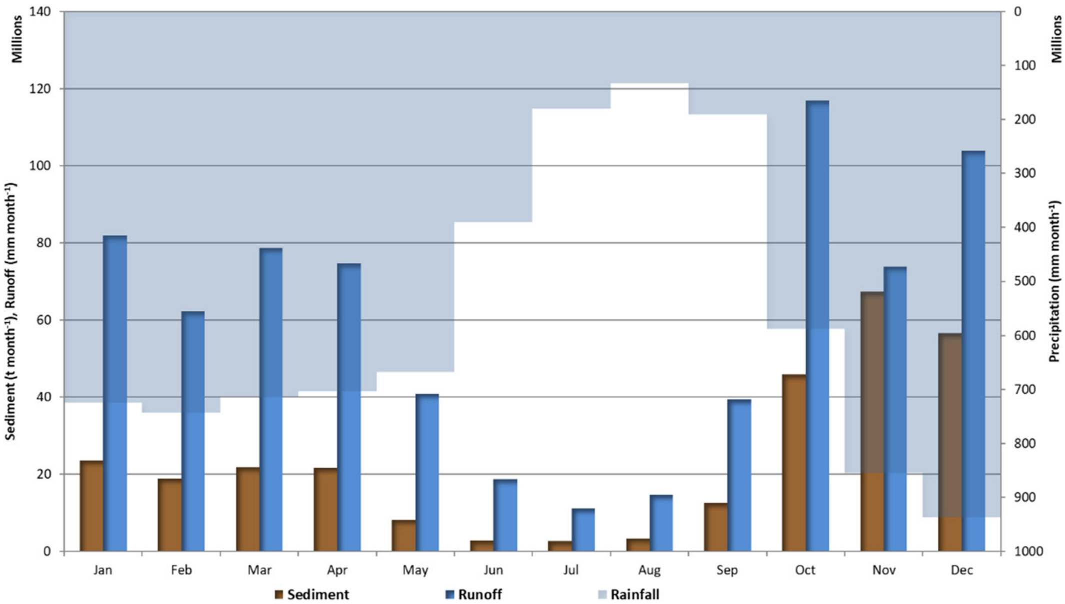

Fig. 10 Monthly distribution of sediment, runoff and precipitation

increase in rainfall that makes the soil more vulnerable. This study showed that the average soil erosion in agricultural areas is expected to decrease under climate change scenarios due to rapid plant biomass production and the increase in the rate of evapotranspiration. In contrast, the average soil erosion in the forest and scrub would increase due to extreme temperature stress and topographic variation.

Conclusion

Sediment transport causes dams to be filled up long before their economic lifetime, thus leading to floods and overflows that cause human and material losses. Land degradation caused by intense erosion may also lead to a substantial decrease in agricultural farming, exacerbating, in return, rural emigrations. In this regard,

Table 6 Monthly soil erosion of Turkey

Months	Monthly erosion				Standard deviation
	($t\ ha^{-1}\ m^{-1}$)			($t\ yr^{-1}$)	
	Min.	Max.	Mean	Total	
January	0	142.75	0.32	23,575,806	1.45
February	0	161.43	0.26	18,859,819	1.48
March	0	448.64	0.30	21,810,031	2.91
April	0	984.07	0.30	21,679,356	3.92
May	0	174.05	0.11	8,229,325	1.07
June	0	89.35	0.04	2,844,919	0.21
July	0	10.38	0.04	2,705,138	0.09
August	0	7.56	0.04	3,270,088	0.12
September	0	55.23	0.17	12,600,081	0.62
October	0	139.24	0.62	45,920,388	1.95
November	0	264.20	0.92	67,288,650	5.23
December	0	347.15	0.77	56,680,950	3.80

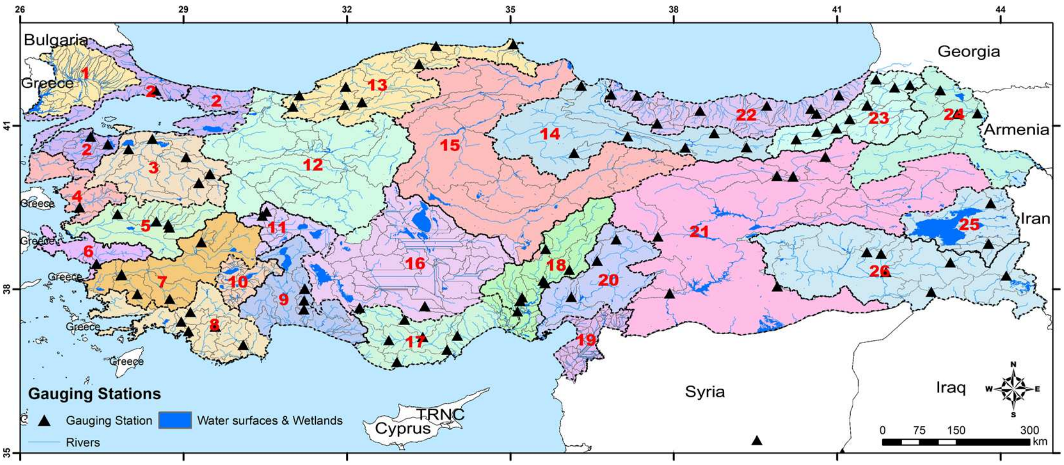

Fig. 11 Location of the gauging stations in each river basin in Turkey

combating erosion should ensure soil conservation, natural resources management and food security.

Land degradation is a severe challenge in Turkey, leading to approximately 255.5 million tonnes of soil loss which threatens 29.45% of agricultural land prone to severe water erosion. The amount of erosion of the Scrublands (11.36 t ha^{-1} yr^{-1}), olive groves (10.06 t ha^{-1} yr^{-1}) and degraded forests (9.95 t ha^{-1} yr^{-1}) was above the mean national soil erosion rate of the country (3.88 t ha^{-1} yr^{-1}). The river basins that experience the highest risk of erosion in Turkey are the sites facing the 70.16% soil loss in the whole of the country with the highest erosion rates determined in degraded forests (101,721,946 t ha^{-1}). The severe risks of erosion the soils of Turkey are facing are due to the inappropriate agricultural practices, stemming from the cultivation of steep lands, excessive soil tillage, hilly topography and soil conditions that accelerate water erosion (i.e. poor plant cover linked to the semi-arid climate and low soil organic matter) (Irvem

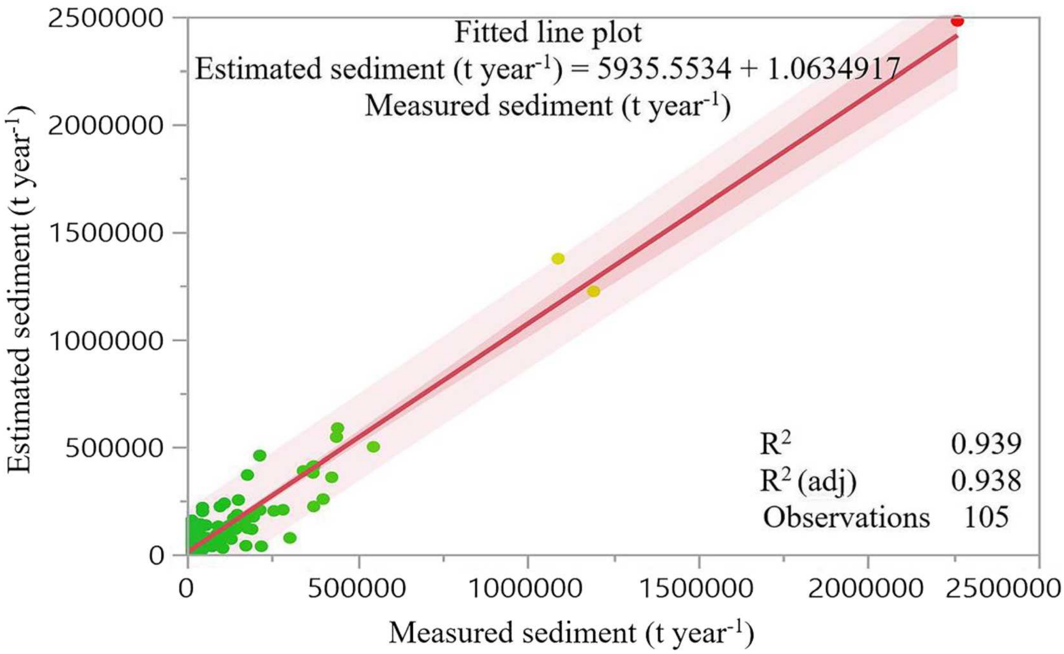

Fig. 12 The fitted line plot for the measured and estimated sediment data

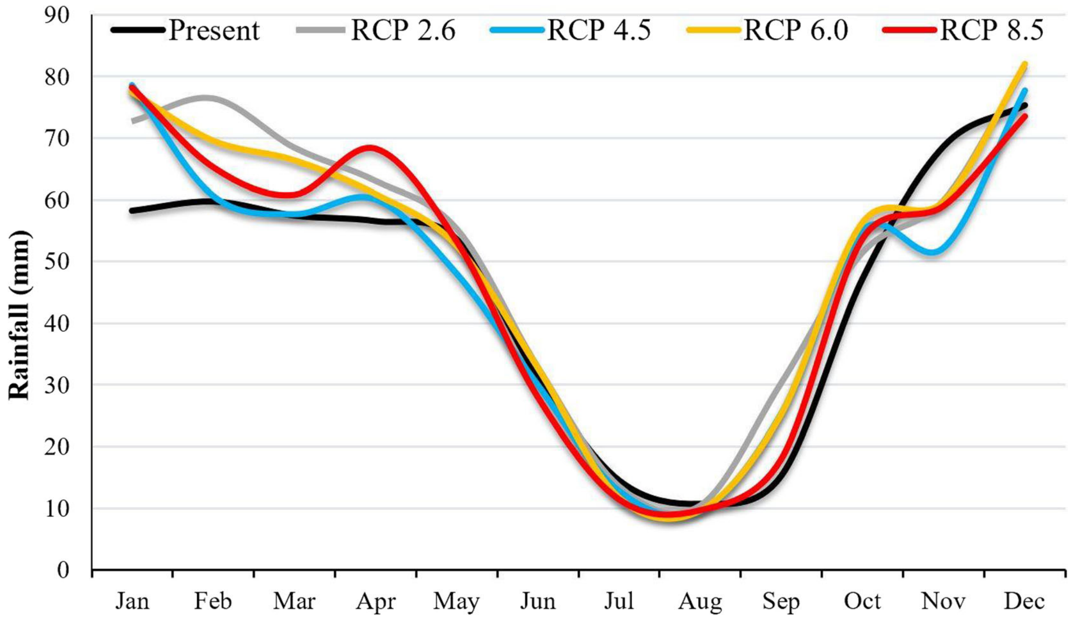

Fig. 13 Distribution of monthly rainfall under climate change scenarios in Turkey

et al. 2007). This extensive challenge threatens the agricultural sustainability of the Mediterranean basins, where various economically significant crops are produced. The Mediterranean soils may be particularly susceptible to global changes due to their poor physical and chemical characteristics, low vegetation cover and fluctuating climatic conditions. Henceforth, it will be essential to understand the possible effects of global change on soil erosion and its impact on the functions of soil, e.g. local water balance, sediment transfer in surface water reservoirs, loss of organic matter (on-site effects) and support of vegetation (Cerdan et al. 2011). A series of intense efforts will be initiated to mitigate the risks and alleviate the damages of desertification, land degradation and drought while human factors are one of the leading drivers of erosion in Turkey. This research resulted in the production of a coherent soil erosion map for Turkey and examined the impact of possible land use and climate changes. The outcomes showed that an incidental effect of climate change may result in a substantial rise in the rate of soil erosion.

It was estimated that the RCP 2.6, RCP 4.5, RCP 6.0 and RCP 8.5 scenarios will result 8%, 13.6%, 12.3% and 24.7% temperature rises for the period from 2060 to 2080, respectively. Erosion from pastures, grassland, heterogeneous cultivated and forest lands will be expected to decrease from 2 to 47%, whereas scrublands will face an increase of 30%. These results indicated that climate change would result in an increase in soil erosion in most of the country due to the changes in the precipitation regime and temperature rise. However, biomass increase as a result of temperature increase and precipitation in some regions will decrease soil erosion. Modelling soil erosion in the long term will enhance our understanding of the spatial variation of soil erosion to device soil conservation schemes. Erosion is particularly expected to decrease at the highlands of north-eastern Turkey. This would be the outcome of the biomass increase in these regions in the future. However, the Mediterranean region would need soil protection due to its high erodibility characteristics accelerated by climate change. Turkey is a good example in embracing diverse topographies, soil properties and misuse of soils, thus, the process-based and multi-attribute model that was used in this study is an appropriate source to be utilised in improving environmental management plans at highly risky land units such as the ones in this country. The analysis of such modelling applications will be useful to help water resource managers in selecting a model based on the

Table 7 The amount of soil erosion for each land cover class considering present and future climate data

Land cover classes	2000–2010		2060–2080							
	Present erosion		Future erosion							
			RCP 2.6		RCP 4.5		RCP 6.0		RCP 8.5	
	Mean (t ha^{-1} yr^{-1})	Total (t yr^{-1})	Mean (t ha^{-1} yr^{-1})	Total (t yr^{-1})	Mean (t ha^{-1} yr^{-1})	Total (t yr^{-1})	Mean (t ha^{-1} yr^{-1})	Total (t yr^{-1})	Mean (t ha^{-1} yr^{-1})	Total (t yr^{-1})
Artificial land	0.99	1,187,967	1.06	1,252,158	0.94	1,119,146	1.02	1,210,554	0.94	1,112,265
Arable land	3.12	55,472,710	3.53	62,741,228	3.37	59,976,012	3.47	61,658,506	3.26	58,055,274
Vineyards	5.90	1,578,919	6.75	1,804,591	6.02	1,610,071	6.40	1,710,169	6.59	1,761,036
Fruit trees and berry plantations	3.06	1,241,661	3.24	1,311,626	2.97	1,202,866	3.15	1,275,389	3.12	1,262,396
Olive groves	10.06	3,648,850	11.19	4,026,290	10.26	3,692,017	11.14	4,006,978	10.76	3,871,440
Pastures and grassland	0.25	2,655,227	0.23	2,349,755	0.18	1,873,138	0.20	2,032,433	0.18	1,887,325
Heterogeneous agricultural land	1.58	19,505,551	1.30	15,999,522	1.07	13,127,155	1.16	14,240,755	1.07	13,144,321
Forest	0.29	3,556,432	0.24	2,911,262	0.23	2,822,181	0.24	2,850,423	0.23	2,821,149
Scrub	11.36	94,922,107	12.90	107,598,870	14.84	123,709,769	14.27	118,991,304	16.73	139,499,307
Bare land	0	0	0	0	0	0	0	0	0	0
Degraded forests	9.95	101,721,496	10.65	108,910,051	11.19	114,348,036	10.99	112,341,023	12.91	131,928,403
Water surfaces and wetland	0	0	0	0	0	0	0	0	0	0
Total	3.88	285,490,920	4.21	308,905,354	4.41	323,480,390	4.36	320,317,534	4.84	355,342,917

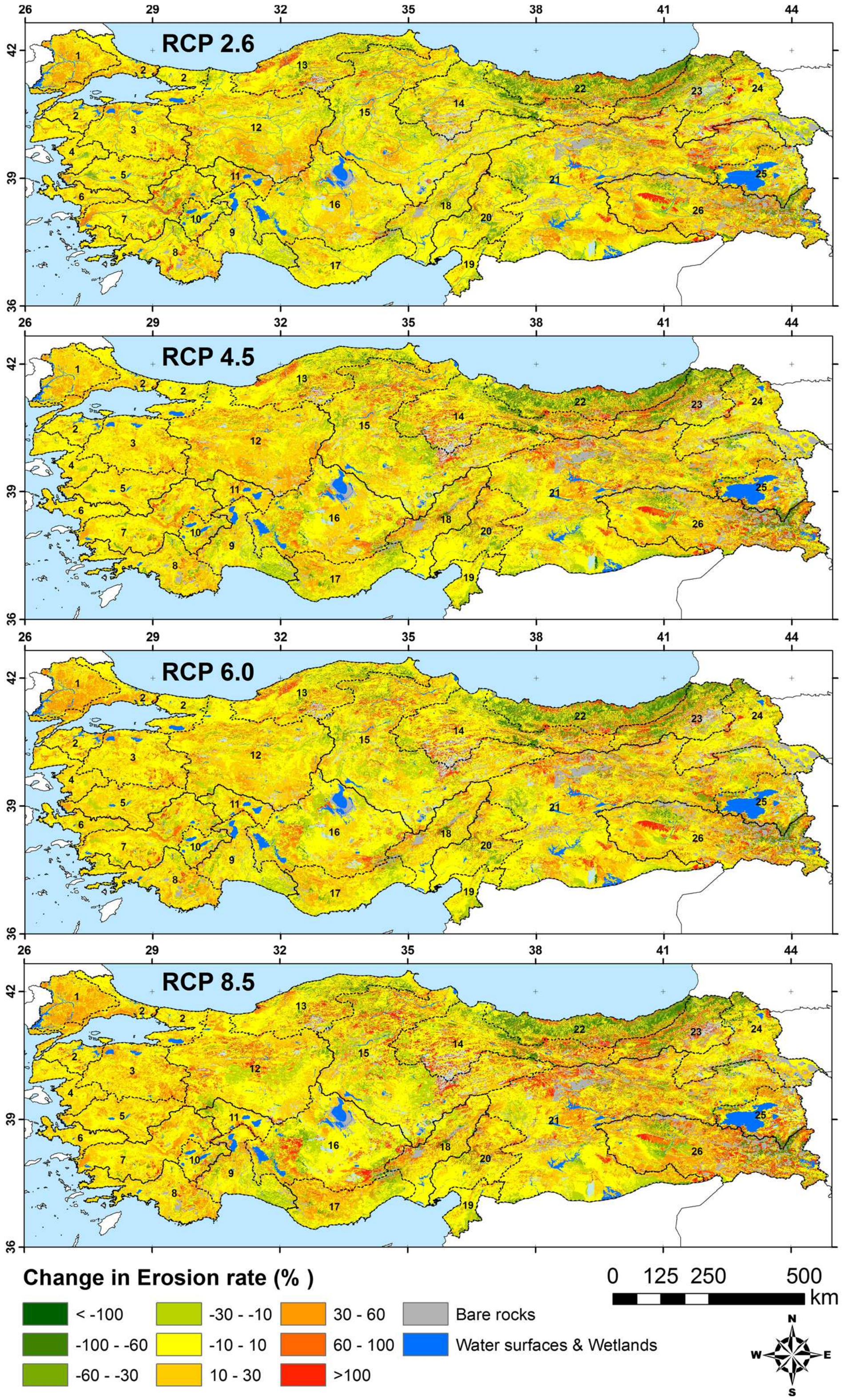

Fig. 14 Change in the soil erosion rate under the four different climate change scenarios

physical characteristics of the watershed and availability of input data.

Acknowledgements This research has been supported by the Scientific Projects Administration Unit of Cukurova University (Project ID: FBA-2019-10983) and the Scientific and Technological Research Council of Turkey (TUBITAK) (Project ID: 110Y338).

References

Abbott, M. B., Bathurst, J. C., Cunge, J. A., O'Connell, P. E., & Rasmussen, J. (1986). An introduction to the European hydrological system — Systeme Hydrologique Europeen, "SHE", 2: Structure of a physically-based, distributed modelling system. *Journal of Hydrology, 87*, 61–77.

Akça, E., Aydin, M., Kapur, S., Kume, T., Nagano, T., Watanabe, T., Çilek, A., & Zorlu, K. (2020). Long-term monitoring of soil salinity in a semi-arid environment of Turkey. *CATENA, 193*, 104614. https://doi.org/10.1016/j.catena.2020.104614.

Amanambu, A. C., Li, L., Egbinola, C. N., Obarein, O. A., Mupenzi, C., & Chen, D. (2019). Spatio-temporal variation in rainfall-runoff erosivity due to climate change in the lower Niger Basin, West Africa. *Catena, 172*, 324–334. https://doi.org/10.1016/j.catena.2018.09.003.

Angima, S., Stott, D., O'Neill, M., et al. (2003). Soil erosion prediction using RUSLE for central Kenyan highland conditions. *Agriculture, Ecosystems and Environment, 97*, 295–308.

Arnhold, S., Lindner, S., Lee, B., Martin, E., Kettering, J., Nguyen, T. T., Koellner, T., Ok, Y. S., & Huwe, B. (2014). Conventional and organic farming: soil erosion and conservation potential for row crop cultivation. *Geoderma, 219–220*, 89–105. https://doi.org/10.1016/j.geoderma.2013.12.023.

Beasley, D., Huggins, L., & Monke, E. (1980). ANSWERS: A model for watershed planning. *Transactions of ASAE, 23*, 0938–0944.

Begum Nasir Ahmad, N. S., Mustafa, F. B., Yusoff, S.@. Y. M., & Gideon, D. (2020). A systematic review of soil erosion control practices on the agricultural land in Asia. *International Soil and Water Conservation Research, 8*, 103–115. https://doi.org/10.1016/j.iswcr.2020.04.001.

Beskow, S., Mello, C. R., Norton, L. D., Curi, N., Viola, M. R., & Avanzi, J. C. (2009). Soil erosion prediction in the Grande River Basin, Brazil using distributed modeling. *Catena, 79*, 49–59. https://doi.org/10.1016/j.catena.2009.05.010.

Boardman, J., Favis-Mortlock, D. T. (2001). How will future climate change and land-use change affect rates of erosion on agricultural land? Soil Eros res 21st century, Proc 498–501.

Brazier, R., Rowan, J., Anthony, S., & Quinn, P. (2001). "MIRSED" towards an MIR approach to modelling hillslope soil erosion at the national scale. *CATENA, 42*, 59–79.

Cerdan, O., Desprats, J. F., Fouche, J., et al (2011). Impact of global changes on soil vulnerability in the Mediterranean Basin. In: International symposium on Erosion and landscape evolution. ASABE publication number 711P0311cd, Anchorage, Alaska, pp 1–8.

Cilek, A. (2017). Soil organic carbon losses by water erosion in a Mediterranean watershed. *Soil Research, 55*, 363.

Cilek, A., Berberoglu, S., Donmez, C., & Unal Cilek, M. (2020). Generation of high-resolution 3-D maps for landscape planning and design using UAV technologies. *The Journal of Digital Landscape Architecture, 5*, 275–284.

CLC (2012). Corine Land Cover 2012. In: Copernicus data Inf. policy Regul. No 1159/2013 12 July 2013. https://www.eea.europa.eu/data-and-maps/data/external/corine-land-cover-2012. Accessed 20 Aug 2008.

Fernández, C., & Vega, J. A. (2016). Evaluation of RUSLE and PESERA models for predicting soil erosion losses in the first year after wildfire in NW Spain. *Geoderma, 273*, 64–72. https://doi.org/10.1016/j.geoderma.2016.03.016.

Finlayson, D. P., & Montgomery, D. R. (2003). Modeling large-scale fluvial erosion in geographic information systems. *Geomorphology, 53*, 147–164.

Fu, B. J., Zhao, W. W., Chen, L. D., Zhang, Q. J., Lü, Y. H., Gulinck, H., & Poesen, J. (2005). Assessment of soil erosion at large watershed scale using RUSLE and GIS: a case study in the Loess Plateau of China. *Land Degradation Development, 16*, 73–85.

Gallaher, R. N., Hawf, L. (1997). Role of conservation tillage in production of a wholesome food supply. In: Gallaher R. (ed) *Proceedings of the 20th annual southern conservation tillage for sustainable agriculture*. University of Florida, Gainesville, pp 23–27.

Gobin, A., Govers, G., Jones, R., et al (2003). Assessment and reporting on soil erosion. Background and workshop report. European Environment Agency 1–103.

Han, F., Ren, L., Zhang, X., & Li, Z. (2016). The WEPP model application in a small watershed in the Loess Plateau. *PLoS One, 11*, 1–11. https://doi.org/10.1371/journal.pone.0148445.

Hijmans, R. J., Cameron, S. E., Parra, J. L., Jones, P. G., & Jarvis, A. (2005). WORLDCLIM - a set of global climate layers (climate grids). *International Journal of Climatology, 25*, 1965–1978.

IPCC Climate Change. (2007). *Climate Change 2007:The physical science basis. Contribution of working group I to the fourth assessment report of the intergovernmental panel on Climate Change*. Cambridge and New York: Cambridge University Press.

Irvem, A., Topaloglu, F., & Uygur, V. (2007). Estimating spatial distribution of soil loss over Seyhan River basin in Turkey. *Journal of Hydrology, 336*, 30–37.

Kirkby, M. J., & Cox, N. J. (1995). A climatic index for soil erosion potential (CSEP) including seasonal and vegetation factors. *Catena, 25*, 333–352.

Kirkby, M. J., Neale, R. H. (1987). *A soil erosion model incorporating seasonal factors*. International Geomorphology, II, John Wiley.

Kirkby, M. J., Le Bissonais, Y., Coulthard, T. J., et al. (2000). The development of land quality indicators for soil degradation by water erosion. *Agriculture, Ecosystems and Environment, 81*, 125–136.

Kirkby, M. J., Gobin, A., Irvine, B. (2003) Pan European Soil Erosion Risk Assessment. Deliverable 5: PESERA model strategy, land use and vegetation growth.

Kirkby, M. J., Jones, R., Irvine, B., et al (2004). Pan-European Soil Erosion Risk Assessment: The PESERA Map, Version 1 October 2003b. Eur soil bur res report off off Publ Eur communities, Luxemb 16:18.

Kirkby, M. J., Irvine, B. J., Jones, R. J. A., Govers, G., & PESERA team. (2008). The PESERA coarse scale erosion model for Europe. I. - model rationale and implementation. *European Journal of Soil Science, 59*, 1293–1306.

Le Bissonnais, Y., Montier, C., Jamagne, M., et al. (2002). Mapping erosion risk for cultivated soil in France. *Catena, 46*, 207–220.

Li, P., Irvine, B., Holden, J., & Mu, X. (2017). Spatial variability of fluvial blanket peat erosion rates for the 21st century modelled using PESERA-PEAT. *Catena, 150*, 302–316. https://doi.org/10.1016/j.catena.2016.11.025.

Merritt, W. S., Letcher, R. A., & Jakeman, A. J. (2003). A review of erosion and sediment transport models. *Environmental Modelling and Software, 18*, 761–799.

Morgan, R. P., Quinton, J. N., Rickson, R. J. (1990). Structure of the soil erosion prediction model for the European community. In: Proceedings of international symposium on water Erosion, Sedimentation and Resource Conservation. Central Soil and Water Conservation Research and Training Institute, CSWCRTI, Dehradun, India, pp 49–59.

Munodawafa, A. (2007). Assessing nutrient losses with soil erosion under different tillage systems and their implications on water quality. *Physics and Chemistry of the Earth, 32*, 1135–1140. https://doi.org/10.1016/j.pce.2007.07.033.

Nazarenko, L., Schmidt, G. A., Miller, R. L., Tausnev, N., Kelley, M., Ruedy, R., Russell, G. L., Aleinov, I., Bauer, M., Bauer, S., Bleck, R., Canuto, V., Cheng, Y., Clune, T. L., del Genio, A. D., Faluvegi, G., Hansen, J. E., Healy, R. J., Kiang, N. Y., Koch, D., Lacis, A. A., LeGrande, A. N., Lerner, J., Lo, K. K., Menon, S., Oinas, V., Perlwitz, J., Puma, M. J., Rind, D., Romanou, A., Sato, M., Shindell, D. T., Sun, S., Tsigaridis, K., Unger, N., Voulgarakis, A., Yao, M. S., & Zhang, J. (2015). Future climate change under RCP emission scenarios with GISS ModelE2. *Journal of Advances in Modeling Earth Systems, 7*, 244–267.

Nearing, M., Foster, G., Lane, L., & Finkner, S. (1989). A process-based soil erosion model for USDA-water erosion prediction project technology. *Transactions of ASAE, 32*, 1587–1593.

Nearing, M., Jetten, V., Baffaut, C., et al. (2005). Modeling response of soil erosion and runoff to changes in precipitation and cover. *Catena, 61*, 131–154.

Ochoa, P. A., Fries, A., Mejía, D., Burneo, J. I., Ruíz-Sinoga, J. D., & Cerdà, A. (2016). Effects of climate, land cover and topography on soil erosion risk in a semiarid basin of the Andes. *Catena, 140*, 31–42. https://doi.org/10.1016/j.catena.2016.01.011.

Panagos, P., Hiederer, R., Van Liedekerke, M., Bampa, F. (2013). Review of the current situation based on data collected through a European network. *Journal of Environmental and Public Health* Artical ID:1–11. https://doi.org/10.1016/j.ecolind.2012.07.020.

Panagos, P., Karydas, C., Ballabio, C., & Gitas, I. (2014). Corrigendum to "Seasonal monitoring of soil erosion at regional scale: an application of the G2 model in Crete focusing on agricultural land uses " [Int. J. Appl. Earth Observ. Geoinform., 27, (2014), 147-155. *International Journal of Applied Earth Observation and Geoinformation, 32*, 240–240. https://doi.org/10.1016/j.jag.2014.04.022.

Renschler, C. S., & Harbor, J. (2002). Soil erosion assessment tools from point to regional scales—the role of geomorphologists in land management research and implementation. *Geomorphology, 47*, 189–209.

Rickson, R. J. (2014). Can control of soil erosion mitigate water pollution by sediments? *The Science of the Total Environment, 468–469*, 1187–1197. https://doi.org/10.1016/j.scitotenv.2013.05.057.

Russell, S. H., & William, W. (2001). *Landscape erosion and evolution modeling*. Boston: Springer US.

Sacks, W. J., Deryng, D., Foley, J. A., Ramankutty, N. (2010). Crop planting dates: an analysis of global patterns. *Global Ecology and Biogeography* 19:No-no. https://doi.org/10.1111/j.1466-8238.2010.00551.x.

Taylor, K. E., Stouffer, R. J., & Meehl, G. A. (2012). An overview of CMIP5 and the experiment design. *Bulletin of the American Meteorological Society, 93*, 485–498.

Terranova, O., Antronico, L., Coscarelli, R., & Iaquinta, P. (2009). Soil erosion risk scenarios in the Mediterranean environment using RUSLE and GIS: an application model for Calabria (southern Italy). *Geomorphology, 112*, 228–245.

Trimble, S. W. (2000). LAND USE: U.S. soil erosion rates–myth and reality. *Science (80-), 289*, 248–250.

TSMS (2012). Climate data, 1975–2012. Turkey: Regional Directorate of State Meteorological Service, Turkish State Meteorological Service. https://www.mgm.gov.tr/. Accessed 24 Aug 2018.

Unal, M., Uslu, C. (2018). Evaluating and optimizing urban green spaces for compact urban areas: Cukurova district in Adana, Turkey. *ISPRS Internal Journal of Geo-Information* 7:. https://doi.org/10.3390/ijgi7020070.

Unal, M., Uslu, C., Cilek, A., & Altunkasa, M. F. (2018). Microclimate analysis for street tree planting in hot and humid cities. *Journal of Digital Landscape Architecture, 3*, 34–42. https://doi.org/10.14627/537642004.

Uzuner, Ç., & Dengiz, O. (2020). Desertification risk assessment in Turkey based on environmentally sensitive areas. *Ecological Indicators, 114*, 106295. https://doi.org/10.1016/j.ecolind.2020.106295.

Vieira, D. C. S., Serpa, D., Nunes, J. P. C., Prats, S. A., Neves, R., & Keizer, J. J. (2018). Predicting the effectiveness of different mulching techniques in reducing post-fire runoff and erosion at plot scale with the RUSLE, MMF and PESERA models. *Environmental Research, 165*, 365–378. https://doi.org/10.1016/j.envres.2018.04.029.

Vinet, L., & Zhedanov, A. (2011). A "missing" family of classical orthogonal polynomials. *Journal of Physics A: Mathematical and Theoretical, 44*, 189–200. https://doi.org/10.1088/1751-8113/44/8/085201.

Wang, F., Li, R., & Yang, Q. K. (2003). Scaling in soil erosion research. *Research of Soil and Water Conservation, 10*, 9–12.

Wicks, J. M., & Bathurst, J. C. (1996). SHESED: a physically based, distributed erosion and sediment yield component for the SHE hydrological modelling system. *Journal of Hydrology, 175*, 213–238.

Wuepper, D., Borrelli, P., & Finger, R. (2020). Countries and the global rate of soil erosion. *Nature Sustainability, 3*, 51–55.

Yang, D., Kanae, S., Oki, T., Koike, T., & Musiake, K. (2003). Global potential soil erosion with reference to land use and climate changes. *Hydrological Processes, 17*, 2913–2928.

Zeng, C., Wang, S., Bai, X., Li, Y., Tian, Y., Li, Y., Wu, L., & Luo, G. (2017). Soil erosion evolution and spatial correlation analysis in a typical karst geomorphology using RUSLE with GIS. *Solid Earth, 8*, 721–736. https://doi.org/10.5194/se-8-721-2017.

Zhang, X., Drake, N., Wainwright, J. (2002). Scaling land surface parameters for global-scale soil erosion estimation. *Water Resources Research* 38:19-1-19–9.

Zobeck, T. M., Parker, N. C., Haskell, S., & Guoding, K. (2000). Scaling up from field to region for wind erosion prediction using a field-scale wind erosion model and GIS. *Agriculture, Ecosystems and Environment, 82*, 247–259.

Publisher's note Springer Nature remains neutral with regard to jurisdictional claims in published maps and institutional affiliations.